A Journal of the Gesellschaft Deutscher Chemiker

Angewandte

GDCh

International Edition

Chemie

www.angewandte.org

Accepted Article

Title: A Manganese Nanosheet: New Cluster Topology and Catalysis

Authors: Axel Jacobi von Wangelin, Uttam Chakraborty, Efrain Reyes-Rodriguez, Serhiy Demeshko, and Franc Meyer

To be cited as: *Angew. Chem. Int. Ed.* 10.1002/anie.201800079
Angew. Chem. 10.1002/ange.201800079

Link to VoR: http://dx.doi.org/10.1002/anie.201800079
http://dx.doi.org/10.1002/ange.201800079

WILEY-VCH

10.1002/anie.201800079

Mn Cluster Catalysis

DOI: 10.1002/anie.200((will be filled in by the editorial staff))

A Manganese Nanosheet: New Cluster Topology and Catalysis

*Uttam Chakraborty,[a,b] Efrain Reyes-Rodriguez,[a] Serhiy Demeshko,[c] Franc Meyer,[c] and Axel Jacobi von Wangelin[a,b]**

***Abstract**: While the coordination chemistry of monometallic complexes and the surface characteristics of larger metal particles are well understood, preparations of molecular metallic nanoclusters remain a great challenge. Discrete planar metal clusters constitute nanoscale snapshots of cluster growth but are especially rare due to the strong preference for three-dimensional structures and rapid aggregation or decomposition. A simple ligand exchange protocol has led to the formation of a novel heteroleptic Mn_6 nanocluster that crystallized in an unprecedented flat chair topology and exhibited unique magnetic and catalytic properties. Magnetic susceptibility studies documented strong electronic communication between the Mn ions. Reductive activation of the molecular Mn_6 cluster enabled catalytic hydrogenations of alkenes, alkynes, and imines.*

Two-dimensional materials have gained a strong foothold in the rapidly developing field of nanoscience. Carbon nanosheets and monolayers of metals and other elements show profoundly different physical properties from the bulk material.[1] Unlike graphene, the possible preparation of transition metal nanosheets are highly challenging due to the lack of convenient metal precursors, the preference for three-dimensional geometries, and the generally high reactivity of metal monolayers.[2] Consequently, only very few examples of small transition metal nanosheets with planar or raft-like arrangements of the metal atoms were reported in the literature. The vast majority of transition metal clusters contains six or more metal atoms in three-dimensional cluster geometries.[3],[4] From a conceptual viewpoint, 3D metal nanoclusters are models of the bulk material. Small 2D metal nanoclusters can be viewed as intermediate stages of the growth of soluble metals or metal ions toward metallic monolayers (Figure 1).[5] Flat metal clusters exhibit unique magnetic properties and distinct catalytic activities due to the electronic, magnetic, and steric communication between the neighbouring metals in the plane. Polynuclear metal carbonyls are by far the most studied class of 2D and 3D clusters which exhibit strong coordination of the CO ligands to the metals, are coordinatively saturated, and thus provide not the best models for metal clusters and surfaces under other, CO-free conditions.[4] An example of a planar CO-free cluster is the oligohydride Rh_7 wheel (type **A**, Figure 1) which contains a planar Rh core that mimics an M(111) monolayer.[3] Recently, Ohki et al. and our group have shown that the reaction of easily available transition metal amide precursor complexes $M\{N(SiMe_3)_2\}_2$ (M = Co, Fe) with commercial hydride sources (diisobutylaluminium hydride, Dibal-H; pinacolborane, HBpin) is a convenient strategy to access new topologies of low-valent transition metal nanoclusters in high yields. Planar Co_4, Co_7 and Fe_4, Fe_6, and Fe_7 clusters have been isolated and characterized. Among the larger metal clusters with six or more metals, the type **A** topology has been realized with Fe and Co, and the truncated wheel of type **B** with Fe.[3] Given the synthetic ease of the formation of the precursors and clusters, the use of simple hydrides as initiators of cluster growth, and the high yields of the resultant nanoclusters, we set out to further explore the potential of such facile procedures for the preparation of carbonyl ligand-free transition metal nanoclusters with new topologies. Here, we report the synthesis of a low-valent manganese nano-sheet with a hitherto unknown arrangement of six Mn atoms in a nearly planar "ladder" architecture (**C**). Magnetic susceptibility measurements support the notion of strong antiferromagnetic interactions between Mn ions resulting in a diamagnetic ground state. The Mn_6 cluster was shown to be a molecular precursor to catalytically active nanoparticles which displayed activities that are distinct from previously reported molecular Mn catalysts.

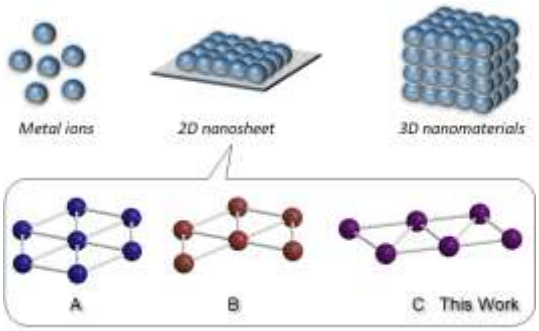

Figure 1. Growth of 2D and 3D transition metal architectures.

Substitution of the bulky amides in $M[N(SiMe_3)_2]_2$ complexes (M = Fe, Co) with hydrides has recently enabled the preparation of soluble Fe and Co nanoclusters.[3] We surmised that an equi-molar reaction of the related manganese complex $Mn[N(SiMe_3)_2]_2$ (**1**)[6] would afford the coordinatively highly unsaturated $[Mn\{N(SiMe_3)_2\}H]$. Oligomerization of this inter-mediate to higher aggregates constitutes a new entry into the nanoscale regime of Mn cluster growth and – in comparison with the related Fe and Co structures - provide new insight into the control of cluster topology by the nature of the 3d transition metal.

[a] Dr. U. Chakraborty, E. Reyes-Rodriguez, Prof. Dr. A. Jacobi von Wangelin*
Dept. of Chemistry, University of Regensburg (Germany)

[b] Prof. Dr. A. Jacobi von Wangelin
Dept. of Chemistry, University of Hamburg
Martin Luther King Pl. 6, 20146 Hamburg (Germany)
E-mail: axel.jacobi@chemie.uni-hamburg.de

[c] Dr. S. Demeshko, Prof. Dr. F. Meyer
University of Göttingen, Institute of Inorganic Chemistry
Tammannstr. 4, D-37077 Göttingen (Germany)

Supporting information for this article is given via a link at the end of the document.

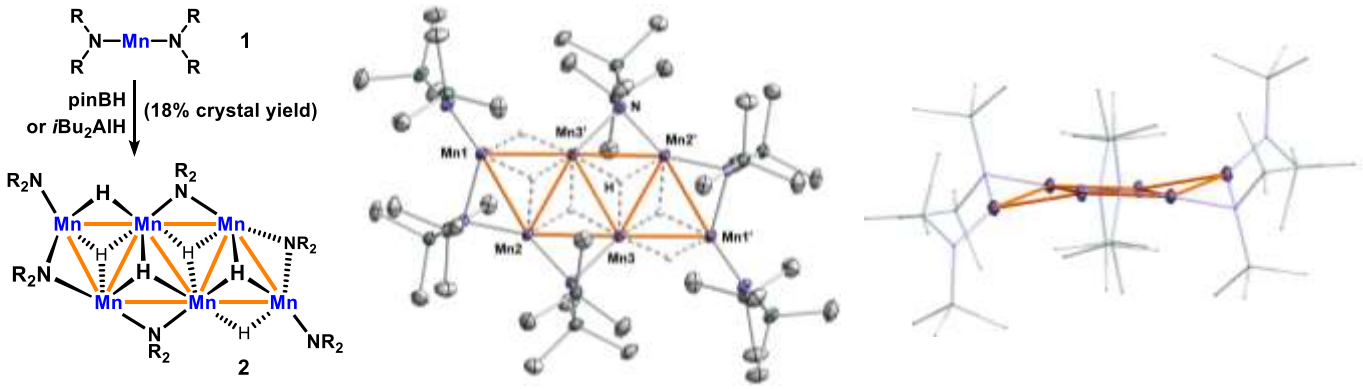

Scheme 1. Synthesis of the Mn_6 cluster **2** (left). Center and right: Crystal structure of **2** (50% probability level, H atoms omitted except for Mn-H).

Paralleling our work with Fe and Co clusters, we were mostly interested in the identification of small soluble nanoclusters that constitute snapshots on the nanoscale of the growth of nanoparticles from low-valent molecular Mn complexes. Indeed, reaction of **1** with 1 equiv. HBpin (or Dibal-H) in *n*-hexane at 20°C readily afforded the novel Mn_6 cluster $[Mn_6(\mu_3\text{-}H)_4(\mu_2\text{-}H)_2\{(\mu_2\text{-}N(SiMe_3)_2\}_4\{N(SiMe_3)_2\}_2]$ as brown single crystals after recrystallization in 18% yield (**2**, Scheme 1). Single crystal structure analysis of **2** displayed an unprecedented "ladder"-type Mn_6 nanocluster containing four μ_2-bridging $N(SiMe_3)_2$ and two terminal $N(SiMe_3)_2$ ligands (Scheme 1, center). The Mn_6 core is best described as a "flat-chair" with four co-planar Mn centers (Mn_2, Mn_3, $Mn_{2'}$ and $Mn_{3'}$). Two Mn centers (Mn_1 and $Mn_{1'}$) cap two opposite edges of the central Mn_4 motif slightly above and below the plane (11.9°) (see Scheme 1, right). Alternatively, this novel near-planar hexametallic architecture can be viewed as an array of four Mn_3 triangles sharing three common edges in a zigzag chain fashion. This structural interpretation could also suggest that the stepwise growth of the Mn_6 nanocluster operates via sequential formal [1+2] additions of Mn_1 units across Mn–Mn bonds. The resultant M_3 triangles are the common topological motif of all members of the $(hmds)_xM_yH_z$ family (hmds = $N(SiMe_3)_2$) with Mn_6, Fe_4, Fe_6, Fe_7, and Co_7 cores.[3] The unprecedented co-planar growth might be a direct consequence of the steric bulk of the hmds ligands which effectively shield the half space above and below the metal plane. The Mn–Mn bond lengths (2.85622(3)–2.97627(3) Å) are in the range of Mn–Mn bonds in other Mn clusters.[7],[11] The positions of the hydride ligands of **2** were located from the electron density Fourier map. Four μ_3-H atoms coordinate the Mn_6 core in alternating up and down fashion. Two μ_2-H atoms span the sterically more hindered peripheral Mn–Mn bonds whereas the least hindered peripheral Mn–Mn edges are coordinated by the bulky hmds ligands.

In an effort to elucidate key properties of **2**, we have further characterized the single crystals. In C_6D_6 solution, **2** is paramagnetic and ^{1}H-NMR silent. Solid **2** is thermally highly stable; no decomposition was observed below 200 °C. The UV-Vis spectrum in *n*-hexane showed a featureless broad band tailing into the visible region (Figure S1). No significant absorption of the Mn–H moiety was detected in the expected region between 1500 and 2000 nm (Figure S2). An effective magnetic moment μ_{eff} of 4.28 μ_B (or 2.29 $cm^3mol^{-1}K$, per Mn_6 cluster, in C_6D_6) was recorded, which is much lower than the spin-only value for six uncoupled S = 5/2 spins (14.49 μ_B or 26.25 $cm^3mol^{-1}K$). This may indicate the presence of strong antiferromagnetic interaction. Thus, the temperature-dependent magnetism was analyzed by a SQUID measurement on solid **2** ($\chi_M T$ vs. T plot in Figure 2). Indeed, $\chi_M T$ drops rapidly and approaches zero at low temperatures, which supports the assumption of strong antiferromagnetic exchange and a diamagnetic ground state. Coupling constants were obtained from fitting the data on the basis of a simplified spin Hamiltonian that includes two coupling constants and Zeeman splitting, using the PHI program.[8] The coupling pattern shown in Figure 2 (inset) was derived from the structural data, where red lines represent coupling through amide and hydride ligands, and blue lines represent couplings only via hydride ligands. For avoiding over-parametrization, *g*-values for all Mn ions were fixed to 2.0. The obtained coupling constants J_A = –40.4 cm^{-1} and J_B = –28.0 cm^{-1} lie in the same range as for trinuclear Mn_3 clusters with comparable Mn–Mn distances.[11e]

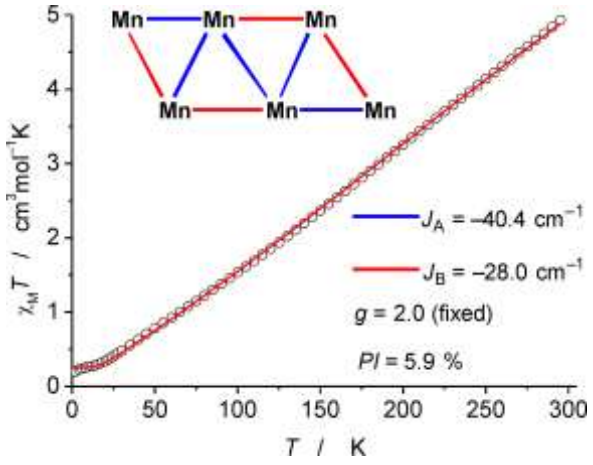

Figure 2. Temperature dependence of $\chi_M T$ for **2**. Solid red line is the best fit (see text and SI for details). Inset: magnetic coupling pattern used for simulation.

Until today, oligonuclear clusters with >5 Mn atoms reported in the literature contained carbonyl and multidentate *N*,*O*-ligands and adopted three-dimensional polyhedral geometries.[7],[9],[10] Two-dimensional Mn clusters are very rare;[11] no carbonyl-free 2D-hexametal skeleton has ever been reported. Two planar Mn_7 wheels of type **A** (Figure 1) are contained within $[Mn][Mn_7(THF)_6(CO)_{12}]_2$ where each $Mn_7(THF)_6(CO)_{12}^-$ anion is coordinated to an isolated Mn^{2+} cation via three carbonyl oxygens to give an octahedral coordination geometry about the central cation.[4] A ladder-type hexametal skeleton was observed in the complex $[Os_6(CO)_{18}(O_2CCF_3)]$.[5] The isolation of the Mn_6 cluster **2**

10.1002/anie.201800079

presents tangible advances over the current state-of-the-art of nanocluster topologies: **2** adopts a rare "flat-chair" geometry of six metal centers; it is free of strongly coordinating CO ligands but contains labile amide and hydride ligands; the linear zigzag cluster growth is distinct from that of the recently reported Fe and Co clusters; the manganese ions show strong antiferromagnetic interactions. Generally, discrete metallic clusters attract great interest due to their special optical, magnetic, and catalytic properties.[12] This first report of an easily accessible, soluble, planar oligo(hydridomanganese) nanosheet has direct ramification for the design and understanding of hydrogen storage materials and hydrogenation catalysts.[3],[13]

An initial survey of the general reactivity pattern of **2** toward various reagents is shown in Scheme 2. Reaction of **2** with 10 equiv. benzaldehyde gave benzylalcohol (55% vs. benzaldehyde) which indicates the presence of >5 active hydride ligands in **2**. The hydride reactivity was insufficient toward the poor electrophiles 4-bromoanisol (no debromination), diphenylacetylene (~1% stilbenes per Mn), and 1-octene. Upon addition of 4-methylpyridine (^{Me}Py, 6 equiv.), the yellow solution of **2** in C_6D_6 afforded a brown solution of a paramagnetic compound exhibiting broad ^{1}H NMR resonances but no free ^{Me}Py. Further addition of ^{Me}Py (12 equiv.) shifted the broad ^{1}H NMR signals towards those of free ^{Me}Py, presumably due to an equilibrium between coordinated and free ^{Me}Py. Addition of 1 equiv. Dibal-H or pinBH to **2** resulted in a black solution presumably due to degradation of the complex to soluble Mn nanoparticles (*vide infra*). The first Mn-catalyzed cyclotrimerization of alkynes was observed. Phenylacetylene was converted to triphenylbenzenes (up to 50% yield) in the presence of 0.83 mol% **2**.[14] Sequential treatment of **2** (1.66 mol%) with ^{Me}Py and pinacolborane (HBpin) gave no hydroboration product, whereas the reverse order of addition (**2**, HBpin, ^{Me}Py) enabled selective 1,2-hydroboration (74% yield). The *in situ* prepared cluster **2** (from $Mn(hmds)_2$, HBpin) exhibited similar hydroboration activity. Hydride transfer appeared to be especially favourable with **2** which prompted us to investigate hydrogenations in the presence of catalytic **2**. Hydrogenations of C=C and C=X bonds have mostly been performed with noble metal catalysts.[16] The use of inexpensive, abundant, and non-toxic base metals has only recently been evaluated in the context of hydrogenations.[17] Manganese, as an early 3d transition metal, has largely been neglected in the development of potential hydrogenation catalysts, despite its high natural abundance (3rd most abundant transition metal in the earth's crust after Fe, Ti) and biocompatibility.[18] In the past three years, only a handful of homogeneous pincer-type Mn complexes were applied to hydrogenations of polar C=X bond systems such as carbonyls, nitriles, and carbon dioxide by the groups of Beller,[19] Kempe,[20] Milstein,[21] and others.[22] On the other hand, Mn-catalyzed hydrogenations of less polar C=X and non-polar C=C bond systems have not been significantly explored.[18] There are two very early examples of the hydrogenation and isomerization of octenes with $Mn_2(CO)_{10}$ under harsh thermal conditions (207 bar H_2, 160 °C)[23] or with *cis*-$(CO)_4(PPh_3)MnH$ under UV light irradiation.[24] The trinuclear carbonyl cluster $[\{Mn(CO)_3\}_3H_3]$[25] was shown to coordinate alkenes and alkynes;[26] however, no further transformations were studied. To the best of our knowledge, there is no report on efficient Mn-catalyzed hydrogenations of less polar unsaturated substrates such as alkenes, alkynes, and imines.

We investigated the hydrogenation of α-methylstyrene (**3**) and 1-phenyl-1-cyclohexene (**4**) under mild conditions (Table 1). The Mn_6 cluster **2** (0.83 mol% = 5 mol% Mn) was inactive at 2 bar H_2 and 20°C, but gave full conversion of **3** at 5 bar H_2 and 60°C. However, the latter conditions led to catalyst precipitation (in *n*-heptane) or rapid colour change from yellow to dark brown (in C_6D_6). Very good catalyst activity at 2 bar H_2 and 20 °C was observed when employing equimolar Dibal-H and **2** (entry 3). The same activity was achieved by *in situ* formation of **2** (from 5 mol% $Mn(hmds)_2$/Dibal-H in *n*-hexane) followed by addition of another 5 mol% of Dibal-H (entry 4). Further optimizations with the more challenging tri-substituted 1-phenyl-1-cyclohexene (**4**) were in full agreement with the fact that the binary catalyst system $Mn(hmds)_2$/Dibal-H (1:2) was the most active hydrogenation catalyst in a non-polar solvent such as *n*-hexane (entry 7). Pinacolborane effected formation of **2** (Scheme 1) but gave an inactive catalyst when mixed with $Mn(hmds)_2$ under the reaction conditions (entries 5, 6). The optimized conditions were applied to hydrogenations of various alkenes (Table 2).

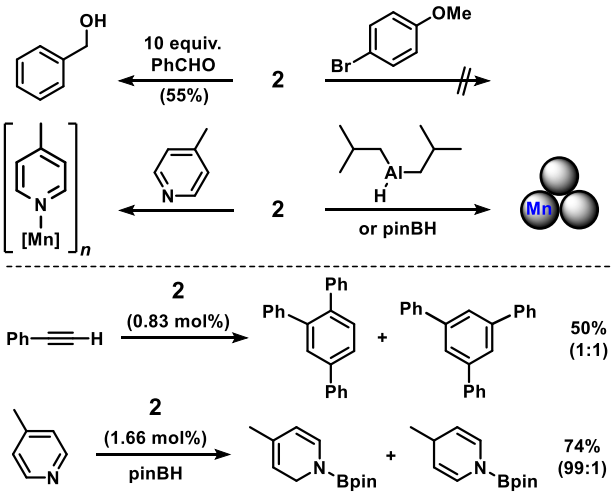

Scheme 2. Survey of stoichiometric (top) and catalytic (bottom) reactions of **2**.

Table 1. Selected optimizations of the Mn-catalyzed alkene hydrogenation.

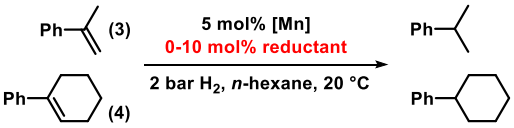

Entry	Catalyst	Reductant (mol%)	Ph-*i*Pr [%]	Ph-Cy [%]
1	**2**	-	0	
2 [a]	**2**	-	100	
3	**2**	*i*Bu$_2$AlH (5)	97	
4 [b]	$Mn(hmds)_2$	*i*Bu$_2$AlH (10)	97	
5	$Mn(hmds)_2$	pinBH (5 or 10)		0
6	$Mn(hmds)_2$	*i*Bu$_2$AlH (5)		0
7	$Mn(hmds)_2$	***i*Bu$_2$AlH (10)**		**>99**
8	$Mn(hmds)_2$	-		0
9 [c]	$MnBr_2$	*i*Bu$_2$AlH (10)		0
10 [d]	$Mn(hmds)_2$	*i*Bu$_2$AlH (10)		2

General conditions: 0.2 mmol alkene, 5 mol% [Mn], reductant, 1 mL hexane, 2 bar H_2 (for **3**), 5 bar H_2 (for **4**), 20 °C, 20 h. [a] 5 bar H_2, 60 °C; [b] *in situ* formation of **2** from $Mn(hmds)_2$ and Dibal-H prior to addition of another 5 mol% Dibal-H; [c] 5 mol% $MnBr_2$ in THF; [d] 5 mol% $MnBr_2$, 10 mol% $LiN(SiMe_3)_2$ in toluene instead of $Mn(hmds)_2$. Yields from quantitative GC-FID vs. internal *n*-pentadecane.

10.1002/anie.201800079

Table 2. Mn-catalyzed hydrogenations of alkenes.

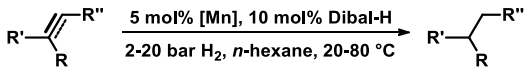

Entry	Alkene	Substituents	Yield [%]
1	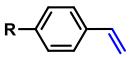	R = H	81
2		R = F	80
3		R = Ph	75
4 [a]		R = *n*-C_5H_{11}	72 (94)
5		R = Me	100
6		R = *n*-Pr	94
7		R = *cyclo*-Pr	91
8		R = Ph	84
9 [b]	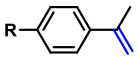	R = F	81 (81)
10 [c]		R = Cl	8 (15)
11		R = Br	0 (0)
12		R = SMe	25 (38)
13		R = OMe	99
14		R = Me	96
15			100
16 [d]	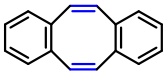		56 (70)
17			76
18 [e]	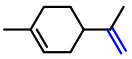		73
19 [f]		R = Me	100
20 [f]		R = Ph	94 (94)
21		n = 1	100
22		n = 2	>99
23		n = 3	45 (47)
24	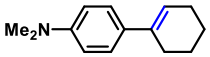		94 (94)
25 [e,g]	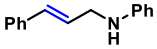		89
26		$R^1 = R^2$ = Ph	96
27		R^1 = Ph, R^2 = Me	77
28		$R^1 = R^2$ = *n*-C_5H_{11}	87

Standard conditions: 0.2 mmol alkene or alkyne, 5 mol% Mn[N(SiMe$_3$)$_2$]$_2$, 10 mol% Dibal-H, hexane, 20 °C; 2 bar H_2, 3 h (entries 1-5); 5 bar H_2, 20 h (entries 6-28). If not otherwise noted, yields were determined by quantitative GC-FID vs. *n*-pentadecane; conversions in parentheses if not >95%; [a] minor isomerization; [b] 5 bar H_2, 3 h. [c] 1% α-methylstyrene formed; [d] mixture of dihydro and tetrahydro products (4:1); [e] isolated yield; [f] 10 bar H_2, *n*-heptane, 60 °C; [g] 20 bar H_2, *n*-heptane, 80 °C.

Mono- and di-substituted alkenes were hydrogenated at 5 bar H_2 and room temperature in very high yields. Turnover frequencies of 65 and 24 h^{-1} were observed in the hydrogenations of 1-octene and α-methylstyrene, respectively at 2 bar H_2, 20 °C after 5 min. The mild reaction conditions tolerated fluoride, thioether, ether, amine, and benzyl functions. Tri-substituted alkenes were quantitatively converted at 10 bar H_2 and 60°C (entries 19-24). Alkynes underwent clean hydrogenation to the alkanes (entries 26-28). A few key mechanistic experiments were performed: No adduct was obtained for the hydrogenation of **3** in the presence of the radical trap triphenylethylene. The catalyst activity was quenched in the presence of ethyl 3,3-dimethylacrylate. Employment of the radical clock α-cyclopropyl styrene led to minor ring opening (9 %) and major hydrogenation (91%).[27] A competitive reaction of 4-methoxy-α-methylstyrene and 4-trifluoromethyl-α-methylstyrene showed more than three times faster hydrogenation of the electron-rich alkene (Scheme 3), which could be explained by the stronger coordination of the better Lewis basic substrate to the catalyst (see also Scheme 1). Following this observation, we extended the scope of the Mn-catalyzed hydrogenation to imines which have not been studied in the literature. Very good conversions were obtained with *N*-aryl and *N*-alkyl aldimines (Table 3). Conjugated styrenyl aldimines underwent highly chemoselective C=N hydrogenation (entries 6-9), which suggests catalyst poisoning by the resulting amine. The higher reactivity of 8-methylquinoline vs. quinoline might also be a direct consequence of unproductive σ-coordination of the latter to the catalyst (entries 11, 12, see Scheme 1).

Table 3. Mn-catalyzed hydrogenations of imines.

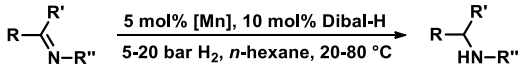

Entry	Imine	Substituents	Yield [%]
1	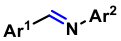	$Ar^1 = Ar^2$ = Ph	93
2		Ar^1 = 4-MeOC_6H_4, Ar^2 = Ph	96
3 [a]		Ar^1 = Ph, Ar^2 = 4-MeSC_6H_4	93
4	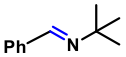		89
5 [b]	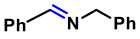		50 (57)
6 [a]		$Ar^1 = Ar^2$ = Ph	96
7 [a,c,d]		Ar^1 = 4-MeOC_6H_4, Ar^2 = Ph	89
8 [a,c,d]		Ar^1 = 4-FC_6H_4, Ar^2 = Ph	83
9 [a,c]		Ar^1 = 4-Me_2NC_6H_4, Ar^2 = Ph	74
10 [a]	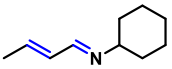		54
11 [a,b]		R = H	11 (18)
12 [a]		R = Me	55
13 [a]	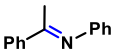		93

Standard conditions: 0.2–0.5 mmol imine, 5 mol% Mn[N(SiMe$_3$)$_2$]$_2$, 10 mol% Dibal-H, *n*-hexane, 5 bar H_2, 20 °C. If not otherwise noted, isolated yields are given; [a] 20 bar H_2, *n*-heptane, 80 °C, 20 h; [b] yields were determined by quantitative GC-FID vs. *n*-pentadecane; conversions in parentheses if not >95%; [c] ~10% alkene hydrogenation; [d] ^{1}H NMR yield.

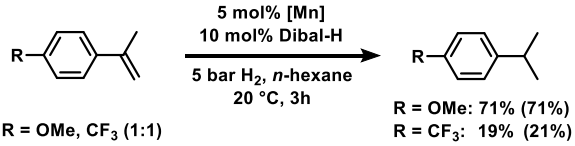

Scheme 3: Competitive hydrogenation of electron-rich vs. electron-poor alkene.

The clear distinction between homogeneous and heterogeneous catalysis mechanisms is not trivial. However, kinetic studies are an instructive tool to discriminate between monometal and cluster catalysts by the analysis of selective poisoning experiments.[28] Addition of "sub-catalytic" amounts of trimethylphosphine at ~30% conversion of α-methylstyrene led to complete catalyst inhibition

already at a catalyst/poison ratio of 5/1 (Scheme S1).[28] Hydrogenation of α-cyclopropyl styrene was only slightly slower in the presence of the homotopic poison dibenzo[*a*,*e*]cyclooctatetraene[29] (dct, 4 equiv. per Mn) which acted as a competing substrate (see SI and entry 16, Table 2). These results are strong indications of a heterotopic reaction mechanism which involves polynuclear low-valent Mn species that form upon reductive activation of the nanocluster **2** with hydride reagents.

In summary, we have reported an unprecedented ladder-type $[XMnH]_6$ cluster that contains bulky amido ligands and active hydrides. This nanosheet complements the small family of planar 3d transition metal clusters and presents a novel cluster topology. The cluster is soluble in organic solvents; its crystals have been studied by X-ray crystallography and solid state SQUID measurements. The latter evidences strong antiferromagnetic exchange interactions and a diamagnetic ground state of **2**. Under reducing conditions, the nanocluster displayed unprecedented catalytic activity in hydrogenations of alkenes, alkynes and imines. Extensions of such nanocluster preparation and applications to small molecule activations are currently being explored.

Acknowledgement

This work was funded by the European Research Council (ERC) through a Consolidator grant (683150). S.D and F.M acknowledge support from the University of Göttingen.

Received: ((will be filled in by the editorial staff))
Published online on ((will be filled in by the editorial staff))

Keywords: manganese · hydrogenations · clusters · hydrides

[1] a) A. J. Mannix, B. Kiraly, M. C. Hersam, N. P. Guisinger, *Nature Rev. Chem.* **2017**, *1*, 0014; b) A. K. Geim, I. V. Grigorieva, *Nature* **2013**, *499*, 419; c) A. K. Geim, K. S. Novoselov, *Nature Mat.* **2007**, *6*, 183.

[2] M. Osada, T. Sasaki, *Adv. Mater.* **2012**, *24*, 210.

[3] Carbonyl-free 2D metal clusters: a) T. N. Gieshoff, U. Chakraborty, M. Villa, A. Jacobi von Wangelin, *Angew. Chem. Int. Ed.* **2017**, *56*, 3585; b) R. Araake, K. Sakadani, M. Tada, Y. Sakai, Y. Ohki, *J. Am. Chem. Soc.* **2017**, *139*, 5596; c) Y. Ohki, Y. Shimizu, R. Araake, M. Tada, W. M. C. Sameera, J.-I. Ito, H. Nishiyama, *Angew. Chem. Int. Ed.* **2016**, *55*, 15821; d) S. K. Brayshaw, J. C. Green, R. Edge, E. J. L. McInnes, P. R. Raithby, J. E. Warren, A. S. Weller, *Angew. Chem. Int. Ed.* **2007**, *46*, 7844; e) E. Cerrada, M. Contel, A. D. Valencia, M. Laguna, T. Gelbrich, M. B. Hursthouse, *Angew. Chem. Int. Ed.* **2000**, *39*, 2353.

[4] 2D metal-CO clusters: a) R. D. Adams, Q. Zhang, X. Yang, *J. Am. Chem. Soc*. **2011**, *133*, 15950 and ref's therein. b) S. Du, B. E. Hodson, P. Lei, T. D. McGrath, F. G. A. Stone, *Inorg. Chem.* **2007**, *46*, 6613; c) G. Kong, G. N. Harakas, B. R. Whittlesey, *J. Am. Chem. Soc.* **1995**, *117*, 3502; d) M. P. Diebold, S. R. Drake, B. F. G. Johnson, J. Lewis, M. McPartlin, H. Powell, *J. Chem. Soc., Chem. Commun.* **1988**, *0*, 1358; e) Doyle, K. A. Eriksen, D. Van Engen, *J. Am. Chem. Soc.* **1986**, *108*, 445.

[5] S. Zacchini, *Eur. J. Inorg. Chem.* **2011**, *2011*, 4125 and ref's therein.

[6] P. P. Power, *Chem. Rev.* **2012**, *112*, 3482.

[7] a) C. E. Holloway, M. Melnik, *J. Organomet. Chem.* **1990**, *396*, 129; b) D. M. P. Mingos, A. S. May, In: *The Chemistry of Metal Cluster Complexes* (Eds.: D. F. Shriver, H. D. Kaesz, R. D. Adams), VCH: New York, **1990**, 11.

[8] N. F. Chilton, R. P. Anderson, L. D. Turner, A. Soncini, K. S. Murray *J. Comput. Chem.* **2013**, *34*, 1164.

[9] A. R. Fout, Q. Zhao, D. J. Xiao, T. A. Betley, *J. Am. Chem. Soc.* **2011**, *133*, 16750.

[10] H. J. Eppley, H.-L. Tsai, N. de Vries, K. Folting, G. Christou, D. N. Hendrickson, *J. Am. Chem. Soc.* **1995**, *117*, 301.

[11] Examples of Mn_3 clusters: a) E. W. Abel, I. D. H. Towle, T. S. Cameron, R. E. Cordes, *J. Chem. Soc., Dalton Trans.* **1979**, 1943; b) P. Legzdins, C. R. Nurse, S. J. Rettig, *J. Am. Chem. Soc.* **1983**, *105*, 3727; c) Z. G. Fang, T. S. A. Hor, K. F. Mok, S. C. Ng, L. K. Liu, Y. S. Wen, *Organometallics* **1993**, *12*, 1009; d) K.-C. Huang, Y.-C. Tsai, G.-H. Lee, S.-M. Peng, M. Shieh, *Inorg. Chem.* **1997**, *36*, 4421; e) A. R. Fout, D. J. Xiao, Q. Zhao, T. D. Harris, E. R. King, E. V. Eames, S.-L. Zheng, T. A. Betley, *Inorg. Chem.* **2012**, *51*, 10290.

[12] a) *Metal Clusters in Catalysis* (Eds.: B. C. Gates, L. Guczi, H. Knözinger), Elsevier: Amsterdam, **1986**; b) H. H. Lamb, B. C. Gates, H. Knözinger, *Angew. Chem., Int. Ed. Engl.* **1988**, *27,* 1127; c) *Metal Clusters in Chemistry* (Eds.: P. Braunstein, L. A. Oro, P. R. Raithby), Wiley-VCH: Weinheim, **1999**; d) E. de Smit, B. M. Weckhuysen, *Chem. Soc. Rev.* **2008**, *37*, 2758. Magnetic applications: e) R. Sessoli, D. Gatteschi, A. Caneschi, M. A. Novak, *Nature* **1993**, *365*, 14; f) R. Sessoli, H. L. Tsai, A. R. Schake, S. Wang, J. B. Vincent, K. Folting, D. Gatteschi, G. Christou, D. N. Hendrickson, *J. Am. Chem. Soc.* **1993**, *115*, 1804; g) D. Gatteschi, R. Sessoli, J. Villain, *Molecular Nanomagnets*, University Press: Oxford, **2006**; h) G. Karotsis, S. J. Teat, W. Wernsdorfer, S. Piligkos, S. J. Dalgarno, E. K. Brechin, *Angew. Chem. Int. Ed.* **2009**, *48*, 8285.

[13] a) T. Shima, Y. Luo, T. Stewart, R. Bau, G. J. McIntyre, S. A. Mason, Z. Hou, *Nat. Chem.* **2011**, *3*, 814; b) R. D. Adams, B. Captain, *Angew. Chem. Int. Ed.* **2008**, *47*, 252; c) A. S. Weller, J. S. McIndoe, *Eur. J. Inorg. Chem.* **2007**, *2007*, 4411; d) J. M. Thomas, R. Raja, B. F. G. Johnson, S. Hermans, M. D. Jones, T. Khimyak, *Ind. Eng. Chem. Res.* **2003**, *42*, 1563.

[14] D. Brenna, M. Villa, T. N. Gieshoff, F. Fischer, M. Hapke, A. Jacobi von Wangelin, *Angew. Chem. Int. Ed.* **2017**, *56*, 8451.

[15] S. Park, S. Chang, *Angew. Chem. Int. Ed.* **2017**, *56*, 7720.

[16] a) *The Handbook of Homogeneous Hydrogenation* (Eds.: J. G. de Vries, C. J. Elsevier), Wiley-VCH: Weinheim, **2007**; b) S. Nishimura, *Handbook of Heterogeneous Catalytic Hydrogenation for Organic Synthesis*; Wiley: New York, **2001**.

[17] a) *Catalysis without Precious Metals* (Ed.: R. M. Bullock), Wiley-VCH: Weinheim, **2010**; b) P. J. Chirik, *Acc. Chem. Res*. **2015**, *48*, 1687; c) K. Junge, K. Schröder, M. Beller, *Chem. Commun*. **2011**, *47*, 4849; d) B. A. F. Le Bailly, S. P. Thomas, *RSC Adv.* **2011**, *1*, 1435.

[18] D. A. Valyaev, G. Lavigne, N. Lugan, *Coord. Chem. Rev.* **2016**, *308*, *Part 2*, 191.

[19] a) S. Elangovan, C. Topf, S. Fischer, H. Jiao, A. Spannenberg, W. Baumann, R. Ludwig, K. Junge, M. Beller, *J. Am. Chem. Soc.* **2016**, *138*, 8809; b) S. Elangovan, M. Garbe, H. Jiao, A. Spannenberg, K. Junge, M. Beller, *Angew. Chem. Int. Ed.* **2016**, *55*, 15364; c) M. Perez, S. Elangovan, A. Spannenberg, K. Junge, M. Beller, *ChemSusChem* **2017**, *10*, 83.

[20] F. Kallmeier, T. Irrgang, T. Dietel, R. Kempe, *Angew. Chem. Int. Ed.* **2016**, *55*, 11806.

[21] N. A. Espinosa-Jalapa, A. Nerush, L. J. W. Shimon, G. Leitus, L. Avram, Y. Ben-David, D. Milstein, *Chem. Eur. J.* **2017**, *23*, 5934.

[22] a) R. van Putten, E. A. Uslamin, M. Garbe, C. Liu, A. Gonzalez-de-Castro, M. Lutz, K. Junge, E. J. M. Hensen, M. Beller, L. Lefort, E. A. Pidko, *Angew. Chem. Int. Ed.* **2017**, *56*, 7531; b) A. Dubey, L. Nencini, R. R. Fayzullin, C. Nervi, J. R. Khusnutdinova, *ACS Catal.* **2017**, 3864; c) F. Kallmeier, R. Kempe, *Angew. Chem. Int. Ed.* **2018**, *57*, 46.

[23] T. A. Weil, S. Metlin, I. Wender, *J. Organomet. Chem.* **1973**, *49*, 227.

[24] P. L. Bogdan, P. J. Sullivan, T. A. Donovan, J. D. Atwood, *J. Organomet. Chem.* **1984**, *269*, c51.

[25] S. W. Kirtley, J. P. Olsen, R. Bau, *J. Am. Chem. Soc.* **1973**, *95*, 4532 and references therein.

[26] R. B. King, M. N. Ackermann, *Inorg. Chem.* **1974**, *13*, 637.

[27] a) R. M. Bullock, E. G. Samsel, *J. Am. Chem. Soc.* **1990**, *112*, 6886; b) J. Masnovi, E. G. Samsel, R. M. Bullock, *J. Chem. Soc., Chem. Commun.* **1989**, 1044.

[28] R. H. Crabtree, *Chem. Rev.* **2012**, *112*, 1536.

[29] a) D. R. Anton, R. H. Crabtree, *Organometallics* **1983**, *2*, 855; b) G. Franck, M. Brill, G. Helmchen, *J. Org. Chem.* **2012**, *89*, 55.

10.1002/anie.201800079

Entry for the Table of Contents

Mn Cluster Catalysis

Uttam Chakraborty, Efrain Reyes-Rodriguez, Serhiy Demeshko, Franc Meyer, and Axel Jacobi von Wangelin*

_____ **Page – Page**

A Manganese Nanosheet: New Cluster Topology and Catalysis

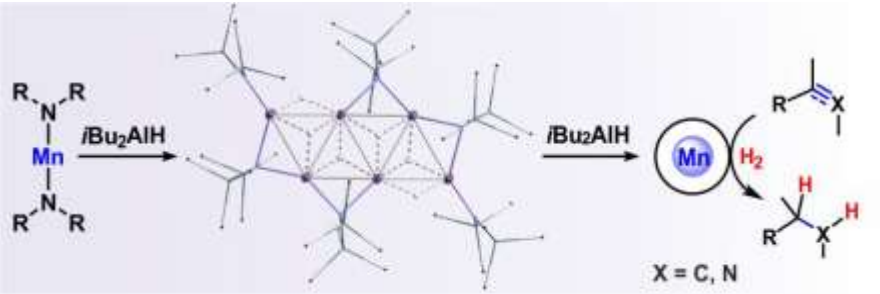

Having six with manganese: An unusual Mn_6 nanosheet has been synthesized from $Mn[N(SiMe_3)_2]_2$ by substitution with boron/aluminium hydrides. Crystallographic characterization documents an unprecedented flat-chair topology; magnetic measurements indicate strong antiferromagnetic coupling and a diamagnetic ground state. Soluble Mn nanoparticles are formed by addition of Dibal-H which constitute the first effective Mn-based catalyst for hydrogenations of alkenes and imines. The isolation of this novel soluble oligohydride-Mn nanocluster provides new insight into the aggregation of molecular complexes to Mn nanoparticles.

10.1002/anie.201800079